

Alkali metal derivatives of an *ortho*-phenylene diamine†

Sarah Robinson , E. Stephen Davies , William Lewis , Alexander J. Blake and Stephen T. Liddle *

School of Chemistry, University of Nottingham, University Park, Nottingham, NG7 2RD, UK. E-mail: stephen.liddle@nottingham.ac.uk

Received 23rd September 2013 , Accepted 29th October 2013

First published on 31st October 2013

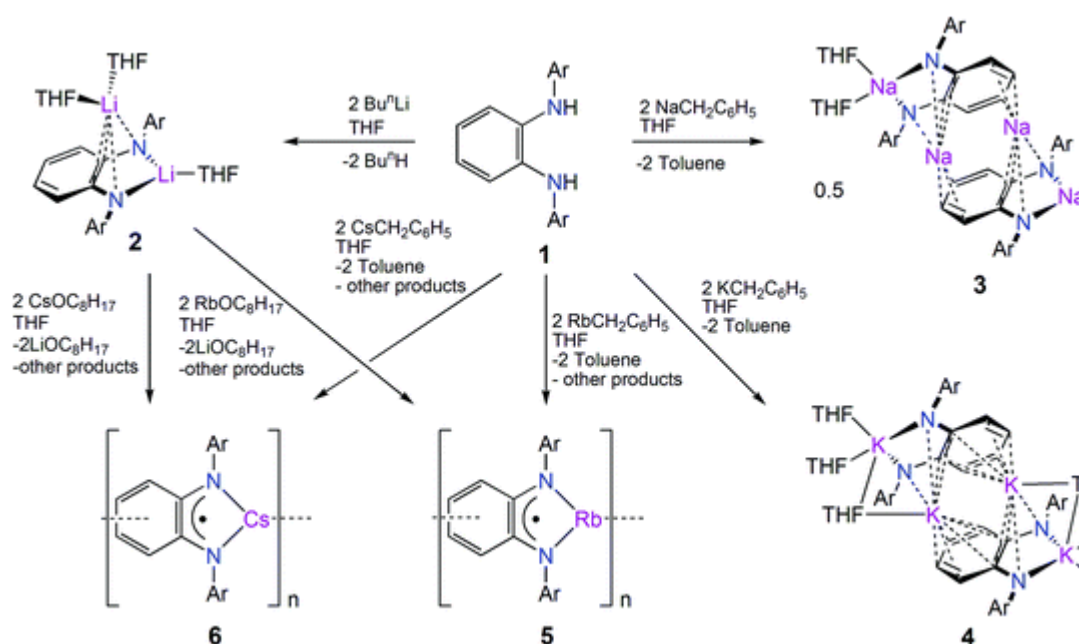
Treatment of the *ortho*-phenylene diamine $C_6H_4-1,2-\{N(H)Tripp\}_2$ (**1**, PDAH₂, Tripp = 2,4,6-triisopropylphenyl) with two equivalents of MR (M = Li, R = Buⁿ; M = Na or K, R = CH₂C₆H₅) afforded the dimetallated alkali metal *ortho*-phenylene diamide dianion complexes [(PDALi₂)(THF)₃] (**2**), [{(PDANa₂)(THF)₂}]₂ (**3**), and [{(PDAK₂)(THF)₃}]₂ (**4**). In contrast, treatment of **2** with two equivalents of rubidium or cesium 2-ethylhexoxide, or treatment of **1** with two equivalents of MR (M = Rb or Cs, R = CH₂C₆H₅) did not afford the anticipated dialkali metal *ortho*-phenylene diamide dianion derivatives and instead formally afforded the monometallic *ortho*-diimino-semiquinonate radical anion species [PDAM] (M = Rb, **5**; M = Cs, **6**). The structure of **2** is monomeric with one lithium coordinated to the two nitrogen centres and the other lithium η⁴-coordinated to the diazabutadiene portion of the PDA scaffold. Similar structural cores are observed for **3** and **4**, except that the larger sodium and potassium ions give dimeric structures linked by multi-hapto interactions from the PDA backbone phenyl ring to an alkali metal centre. Complex **5** was not characterised in the solid state, but the structure of **6** reveals coordination of cesium ions to both PDA amide centres and multi-hapto interactions to a PDA backbone phenyl ring in the next unit to generate a one-dimensional polymer. Complexes **2**–**6** have been variously characterised by X-ray crystallography, multi-nuclear NMR, FTIR, and EPR spectroscopies, and CHN microanalyses.

Introduction

ortho-Phenylene diamines (PDAH₂) are excellent pro-ligands for the synthesis of main group and transition metal derivatives.¹⁻⁹ Although in principle these compounds often undergo straightforward double deprotonation to afford the corresponding *ortho*-phenylene diamide dianions (PDA²⁻), it is known that PDA derivatives can be redox-active, non-innocent compounds resulting in the formation of *ortho*-diiminosemiquinonate radical anions (PDA^{1-•}) or even neutral *ortho*-benzoquinonediimines (PDA⁰).^{10,11} Nevertheless, PDA²⁻ dianions are potentially useful ligands due to the facile variation of the *N*-substituents. In recent years, a significant use for the PDA framework has been the stabilisation of boryl anions.¹²⁻¹⁷ Most PDA-stabilised boryl anions employ *N*-Dipp substituents (Dipp = 2,6-diisopropylphenyl),¹⁸ but recently we reported a *N*-Tripp PDAH₂ variant C₆H₄-1,2-{N(H)Tripp}₂ (**1**, PDAH₂, Tripp = 2,4,6-triisopropylphenyl) which can be used to prepare a bromo-borane derivative PDABBr.¹⁹ The PDA bromo-borane can be converted to a lithium boryl derivative, effect alkali metal-mediated 2- and 2,6-borylations of naphthalene, or be used to directly access the corresponding hydroborane.¹⁹ The PDA bromo-borane derivative is prepared by reaction of PDAH₂ with BBr₃ and CaH₂, but unfortunately this reaction only yields PDABBr in 44% isolated yield despite attempts to optimise the yield. We therefore investigated alternative PDA²⁻ transfer reagents and targeted dialkali metal derivatives over the whole of group 1 since structurally authenticated alkali metal PDA derivatives are currently limited to lithium. Herein, we report our endeavours in this area resulting in dilithium, -sodium, and -potassium PDA²⁻ derivatives, and the unexpected formation of monorubidium and -cesium PDA^{1-•} radical anions as confirmed by EPR spectroscopy.

Results and discussion

Addition of two equivalents of *n*-butyl lithium to **1** in THF afforded [(PDALi₂)(THF)₃] (**2**) in 94% yield as a free-flowing yellow-green powder after work-up (Scheme 1). The ¹H NMR spectrum of **2** is devoid of the characteristic singlet resonance at 5.3 ppm that corresponds to the amine protons of **1**, therefore implying complete conversion of **1** to **2**. In addition, the ¹H NMR spectrum of **2** exhibits two sets of *ortho*-isopropyl methyl resonances indicating hindered rotation that places one methyl group close to the PDA phenyl backbone whereas the other methyl group points in the opposite direction. The ⁷Li NMR spectrum of **2** in C₆D₆ exhibits a singlet resonance at 1.6 ppm, suggesting that the two lithium atoms are equivalent in solution.



Scheme 1 Synthesis of 1–6. Ar = 2,4,6-triisopropylphenyl.

Yellow-green crystals of **2** suitable for X-ray crystallographic analysis were isolated from THF at $-30\text{ }^{\circ}\text{C}$ and the molecular structure of **2** is illustrated in Fig. 1 with selected bond lengths and angles in Table 1. Compound **2** crystallises in the monoclinic space group Cc . The unit cell contains four molecules of **2** and eight THF solvent molecules. Compound **2** is monomeric in the solid state and the PDA ligand coordinates to the two lithium cations through its nitrogen atoms, generating two five-membered rings which are highly puckered about the $\text{N}\cdots\text{N}$ vector. The Li2 centre lies essentially in the plane of the PDA backbone, whilst Li1 lies out of the plane of the molecule and is η^4 -coordinated to the diazabutadiene portion of the PDA scaffold. The Li2–N1 and Li2–N2 bond distances of 1.942(4) and 1.982(4) Å, respectively, are significantly shorter than those for Li1–N1 and Li1–N2 [2.077(4) and 2.131(4) Å, respectively], which is consistent with the fact that Li1 is coordinated to the π -system out of the plane of the molecule [Li(1) \cdots C(1) 2.492(4), Li(1) \cdots C(6) 2.462(4) Å]. Despite this, all the Li–N bond lengths are in the normal range observed for Li–N_(amido) bonds (1.89–2.16 Å),²⁰ and compare well to those observed in the *N*-Dipp analogue of **2**.¹² The coordination sphere of each lithium ion is completed by THF molecules (two for Li1, one for Li2). Thus, the coordination geometry around Li2 is best considered as a slightly distorted trigonal planar arrangement ($\sum\angle = 358.7^{\circ}$), whereas Li1 adopts a distorted tetrahedral geometry. The structure of **2** is similar to dilithium *N,N'*-disilyl-*ortho*-phenylene diamides,^{21,22} but different to the recently reported *N*-Dipp analogue²³ of **2** which can be attributed to the steric demands of Tripp *versus* Dipp.

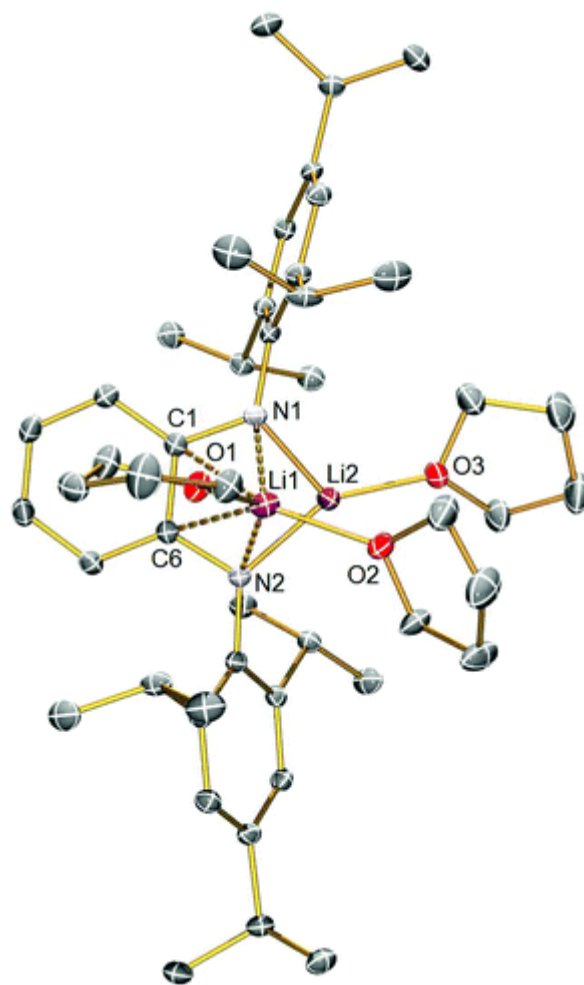


Fig. 1 Molecular structure of **2** with displacement ellipsoids set to 40% and selective labelling. Hydrogen atoms and other components omitted for clarity.

Table 1 Selected bond lengths (Å) and angles (°) for **2**

Li1–N1	2.077(4)
Li1–N2	2.131(4)
Li2–N1	1.942(4)
Li2–N2	1.982(4)
Li1–O1	1.947(4)
Li1–O3	1.999(4)
Li2–O4	1.899(4)
Li1···C1	2.492(4)
Li1···C6	2.462(4)
N1–C1	1.396(3)
N2–C6	1.395(3)
N1–C7	1.411(2)
N2–C22	1.412(2)
Li1–N1–C1	34.53(9)
Li1–N2–C6	33.99(9)

Li2–N1–C1 30.02(9)
Li2–N2–C6 29.82(9)
N1–Li1–N2 77.78(14)
N1–Li2–N2 84.64(16)
N1–Li1–O1 116.85(19)
N1–Li1–O3 116.5(2)
N1–Li2–O4 122.1(2)
N2–Li2–O4 152.0(2)

After stirring **1** with two equivalents of benzylnsodium for 24 hours at ambient temperature in THF, $[\{(\text{PDANa}_2)(\text{THF})_2\}_2]$ (**3**) was isolated from toluene at $-30\text{ }^\circ\text{C}$ as orange crystals ([Scheme 1](#)). The ^1H NMR spectrum of **3** in d_8 -THF is relatively complex, suggesting that the dimeric formulation observed in the solid state is maintained in solution (*vide infra*). Five broad, poorly resolved and overlapping doublets corresponding to the isopropyl- CH_3 groups in a 1 : 2 : 1 : 1 : 1 integral ratio are observed, implying hindered rotation about the *ortho*-isopropyl groups. In contrast to the symmetric nature of **2** in solution, the presence of five doublets suggests that the disodium salt **10** is asymmetric, with the two sodium atoms being inequivalent in solution. This asymmetry can be attributed to the dimeric nature of the compound, essentially affording a ‘front’ and a ‘back’ methyl environment for the *ortho*-isopropyl groups, in addition to the ‘top’ and the ‘bottom’ methyl environments observed for **2**. As a result of their *para*-positions, the *para*-isopropyl CH_3 groups would be expected to experience no steric restrictions, thus displaying free rotation affording a resonance twice as intense as those corresponding to the *ortho*-isopropyl CH_3 groups. Complex **3** exhibits extremely poor solubility, even in polar solvents once isolated. This poor solubility precluded variable temperature NMR experiments.

Compound **3** crystallises in moderate yield (24%) as orange blocks in the monoclinic space group $P2_1/c$. The unit cell contains two molecules of **3**. Four solvent THF molecules act to stabilise the complex by coordinating to two of the sodium atoms. Selected bond lengths and angles are listed in [Table 2](#). Complex **3** crystallises as a centrosymmetric dimer, featuring two distinct sodium environments ([Fig. 2](#)), in a structure that is similar to dimeric $[\{\text{C}_6\text{H}_4(\text{NCH}_2\text{Bu}')_2\text{Li}_2(\text{THF})_2\}_2]$.²¹ Both unique sodium atoms are coordinated to the nitrogen atoms of the PDA ligand, resulting in the generation of two five-membered chelate rings. In a similar manner to that observed in **2**, one of the sodium atoms (Na1) lies within the plane of the PDA

core, whereas Na2 lies out of the plane. The coordination geometries of the two sodium atoms are also very different. The coordination sphere of Na1 is supplemented by two coordinated THF solvent molecules, whereas that of Na2 is completed by five short Na \cdots C_(aryl) interactions; three with the aryl carbon atoms of the six-membered aromatic backbone of the symmetry equivalent of the ligand [Na2 \cdots C3A 2.7922(19), Na2 \cdots C4A 2.6453(19), Na2 \cdots C5A 2.9035(19) Å], and two with the aromatic backbone of the original ligand [Na2 \cdots C1 2.7398(18), Na2 \cdots C2 2.7020(18) Å]. This results in the combination of two multi-hapto interactions, η^3 and η^2 , respectively. The presence of additional short Na \cdots C_(aryl) interactions in compound **3** compared to **2**, can be attributed to the increase in ionic radius of sodium (0.98 Å) compared to lithium (0.78 Å).⁴ The Na2–N1 and Na2–N2 bond distances of 2.4549(16) and 2.4153(16) Å, respectively, are slightly longer than those for Na1–N1 and Na1–N2 [2.3788(18) and 2.3923(15) Å, respectively]. This is consistent with the fact that Na2 lies out of the PDA backbone plane. The Na–O bond distances of 2.314(5) and 2.190(5) Å are comparable to the range reported for the similar dimeric sodium compound, {Na₂(LH₃)₂[(CH₃)₂CO]₃}·2CHCl₃·2H₂O (L = calix[4]arene) [2.280(5)–2.518(6) Å],²⁴ and are close to the sum of the covalent radii for sodium and oxygen (2.18 Å).²⁵ These bond distances also compare well to similar Na–O_(THF) bond distances in [Na{HC(PPh₂NAd)₂}(THF)₂] (Ad = adamantyl) [2.3924(12) and 2.3495(12) Å].²⁶

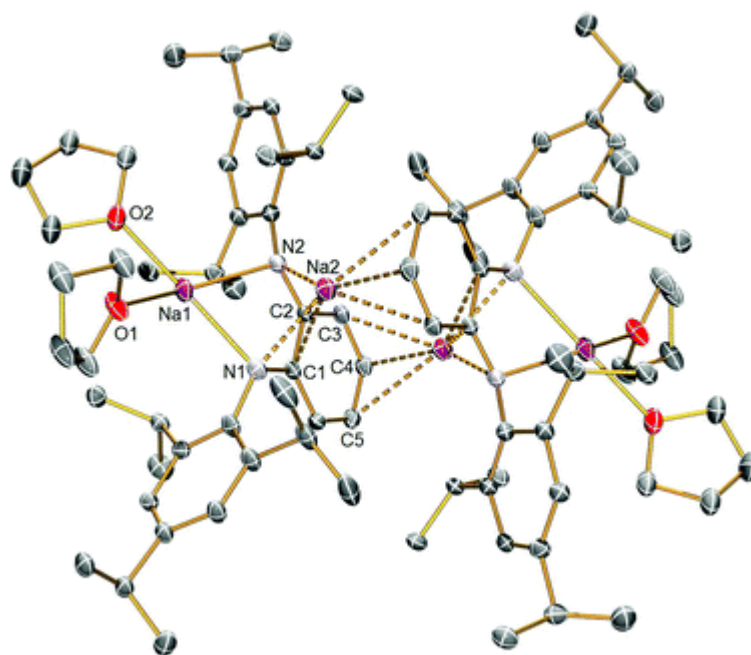


Fig. 2 Molecular structure of **3** with displacement ellipsoids set to 40% and selective labelling. Hydrogen atoms omitted for clarity.

Table 2 Selected bond lengths (Å) and angles (°) for **3**

Na1–N1	2.3788(18)
Na1–N2	2.3923(15)
Na2–N1	2.4549(16)
Na2–N2	2.4153(16)
Na1–O1	2.314(5)
Na1–O2	2.190(5)
Na2···C3A	2.7922(19)
Na2···C4A	2.6453(19)
Na2···C5A	2.9035(19)
Na2···C1	2.7398(18)
Na2···C2	2.7020(18)
N1–C1	1.372(2)
N2–C2	1.377(2)
N1–C7	1.414(6)
N2–C22	1.411(10)
Na1–N1–C1	24.37(5)
Na1–N2–C2	109.83(10)
Na2–N1–C1	86.56(10)
Na2–N2–C2	86.30(10)
N1–Na1–N2	69.22(5)
N1–Na2–N2	67.61(5)
N1–Na1–O1	102.4(2)
N2–Na1–O2	111.35(19)

Analogously to **3**, treatment of **1** with two equivalents of benzyl potassium afforded $[(\text{PDAK}_2)(\text{THF})_3]_2$ (**4**) in 67% yield as green crystals (Scheme 1). The NMR data for complex **4** (d_8 -THF) are largely comparable to those for the analogous sodium compound **3**, and like **3** suggest that the dimeric structure observed in the solid state persists in solution. Again, five broad, overlapping doublet resonances (integral ratio = 1 : 1 : 1 : 2 : 1) are observed in the ^1H NMR spectrum, indicating restricted rotation of the *ortho*-isopropyl groups, but these are not as well resolved as for **3**. Interestingly, however, the ^1H NMR spectrum of **4** is simpler than for **3**, which may reflect the more symmetrical nature of **4**, arising from the even number of multi-hapto interactions (η^6) occurring within the compound, compared to **3**. Similarly to **3**, **4** is very insoluble once isolated, even in polar solvents, which precluded variable temperature NMR experiments.

In gross terms the structure of **4** is analogous to **3** and crystallises as a centrosymmetric dimer in the monoclinic space group $P2_1/c$ (Fig. 3 and Table 3). The two unique potassium ions are bound by the N1 and N2 atoms of the ligand, generating two five-membered chelate rings. Similarly to **2** and **3**, one of the metal ions [K1] in **4** lies out of the plane of the five-membered ring and is η^4 -coordinated to the diazabutadiene fragment [K1 \cdots C1 3.170(6), K1 \cdots C6 3.188(6) Å], whereas the other [K2] lies in the plane of the PDA core. Three molecules of THF coordinate to K2, rendering it five-coordinate, and one of these THF molecules bridges to K1. The coordination environment of K1 is supplemented by the presence of six short K \cdots C_(aryl) interactions with the carbon atoms of the six-membered aromatic backbone of the symmetry equivalent ligand, resulting in an η^6 -interaction [K1 \cdots C1A 3.314(6), K1 \cdots C2A 3.180(6), K1 \cdots C3A 3.046(6), K1 \cdots C4A 2.982(6), K1 \cdots C5A 3.018(6), K1 \cdots C6A 3.234(6) Å] which compares well to other examples of η^6 -arene potassium interactions.^{27–33} This increase in both the number of coordinated solvent molecules and the number of multi-hapto interactions in **4** is consistent with the increase in ionic radius of potassium (1.33 Å) compared to sodium (0.98 Å).³³ The K2–N1 and K2–N2 bond distances of 2.801(5) and 2.763(6) Å, respectively, are slightly longer than those for K1–N1 and K1–N2 [2.729(5) and 2.759(5) Å, respectively]. This is not consistent with the lengthening of the out-of-plane M–N bonds observed for the analogous dilithium (**2**) and disodium (**3**) compounds, and can possibly be attributed to the increase in number of coordinated solvent molecules on K2. However, all K–N bond lengths are consistent with K–N distances reported in similar compounds. For example, the K–N distances in [*o*-{N(SiMe₃)C(^tBu)–C(H)}₂C₆H₄]{K₂(TMEDA)}_n range from 2.776(19) to 2.950(17) Å.³⁴ The K–O_(THF) bond lengths of 2.773(5), 3.040(5) and 2.738(5) Å are slightly longer than the sum of the covalent radii of potassium and oxygen (2.59 Å),³³ and compare well to similar K–O_(THF) bond distances: [K{HC(PPh₂NAd)₂}(THF)₂] [2.6840(12) and 2.8804(12) Å].²⁶

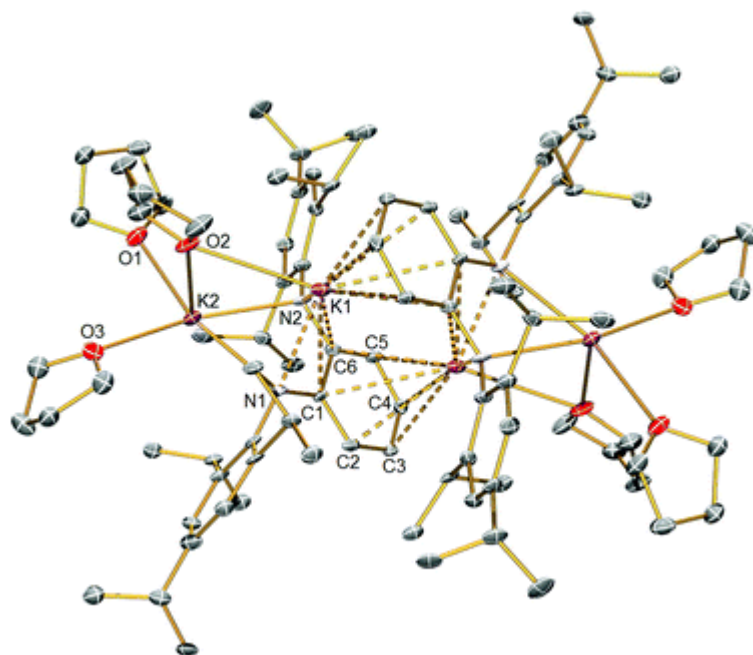


Fig. 3 Molecular structure of **4** with displacement ellipsoids set to 40% and selective labelling. Hydrogen atoms and other components omitted for clarity.

Table 3 Selected bond lengths (Å) and angles (°) for **4**

K1–N1	2.729(5)
K1–N2	2.759(5)
K2–N1	2.801(5)
K2–N2	2.763(6)
K2–O1	2.773(5)
K2–O2	3.040(5)
K2–O3	2.738(5)
K1···C1	3.170(6)
K1···C6	3.188(6)
K1···C1A	3.314(6)
K1···C2A	3.180(6)
K1···C3A	3.046(6)
K1···C4A	2.982(6)
K1···C5A	3.018(6)
K1···C6A	3.234(6)
N1–C1	1.391(8)
N2–C6	1.397(8)
N1–C7	1.388(8)
N2–C22	1.386(8)
K1–N1–C1	25.92(15)
K1–N2–C6	25.91(14)
K2–N1–C1	110.9(3)
K2–N2–C6	113.6(4)

N1–K1–N2 61.31(15)
N1–K2–N2 60.38(15)
N2–K2–O1 101.71(15)
N2–K2–O2 100.49(14)
N2–K2–O3 165.78(15)

The heavier group 1 metals rubidium and cesium are predicted to be more labile than their lighter counterparts as a consequence of the fact that the Rb^+ and Cs^+ ions are larger, more electropositive and hence polarisable [Rb^+ (1.49 Å) and Cs^+ (1.65 Å); compared to Li^+ (0.78 Å), Na^+ (0.98 Å) and K^+ (1.33 Å)].³³ As a result, the dirubidium and -cesium salts of PDA were postulated to be more reactive than their lighter counterparts (**2–4**). Heavy group 1 metal complexes are still generally rare yet have proven to be valuable ligand transfer reagents where the lighter alkali metal derivatives fail.^{26,35,36} We thus identified the dirubidium and -cesium derivatives of **1** as desirable compounds to have in hand for the preparation of PDABBr. Reaction of the dilithium salt **2** with rubidium 2-ethylhexoxide was anticipated to afford the analogous dirubidium salt by metathesis.

After stirring a mixture of **2** and two equivalents of rubidium 2-ethylhexoxide at ambient temperature for 24 hours, a viscous green oil was obtained after work-up ([Scheme 1](#)). Analysis of the green oil by ^1H and ^{13}C NMR spectroscopy proved to be uninformative due to the presence of broad resonances. However, ^7Li NMR spectroscopy suggested that no lithium-containing species remained in the reaction mixture. Despite exhaustive recrystallisation attempts, only polycrystalline material was obtained. Whilst the isolation of an oil could be an indication that a mixture of products was in fact formed, it could also indicate that the product does not contain an ideal metal size to ligand ratio for optimal crystal growth.³⁷ This would be a feasible explanation as the ionic radii of the group 1 metals vary over a 0.87 Å range,³³ and it is therefore quite possible that the larger elements in the series are too large to form the corresponding dimetallic salts. Based on the redox-active proclivity of PDA derivatives,^{10,11} reports of paramagnetic diazabutadiene complexes,^{38,39} and the significant broadening of the NMR resonances observed for the product, we postulated that a paramagnetic rubidium compound [PDARb] (**5**) was formed. We therefore attempted to prepare a dirubidium PDA derivative by a deprotonation strategy.

Accordingly, we treated **1** with two equivalents of benzyl rubidium, and after stirring the reaction mixture for 24 hours at room temperature, a viscous yellow-green oil was isolated after work-up (Scheme 1). Again, all attempts to grow X-ray quality crystals failed and NMR spectra were broad and uninformative, but compared well to those observed for the metathesis reaction. For reasons discussed previously, it is postulated that instead of preparing the anticipated dirubidium PDA complex, the monorubidium salt **5** is formed.

Analogously to **5**, reaction of **2** with cesium 2-ethylhexoxide or treatment of **1** with two equivalents of benzyl cesium afforded an emerald green oil. Again, NMR spectroscopy proved uninformative due to the presence of broad resonances. It was therefore surmised that the monocesium salt [PDACs] (**6**) had been formed. Gratifyingly, after stirring the reaction mixture for 12 hours at ambient temperature in THF, colourless crystals of **6** were isolated in 57% yield from toluene at $-30\text{ }^{\circ}\text{C}$ which proved amenable to interrogation by X-ray crystallography.

Complex **6** crystallises in the orthorhombic space group *Pnma* (Fig. 4 and Table 4). A crystallographic mirror plane bisects the molecule through the centre of the benzene and diazabutadiene portions of the PDA backbone, rendering the N–Cs bonds identical within the molecule. The two nitrogen atoms are three-coordinate, exhibiting a distorted trigonal planar geometry ($\sum\angle = 360^{\circ}$). The Cs1–N1 bond length of 2.985(9) Å compares to that observed in the monocesium compounds, [Cs(LH₃)(py)]_n (L = calix[4]arene) [3.098(16) Å],²⁴ [Cs{([Me₃Si]₂C)P(C₆H₄CH₂NMe₂)₂}(toluene)]_n [3.2758(19) and 3.1039(17) Å],³⁵ and the amide-bridged dimeric complex [Cs(μ-TMP)(TMEDA)]₂ [Cs–N = 3.198(2) Å, TMP = 2,2,6,6-tetramethylpiperidide],⁴⁰ and is close to the sum of the covalent radii of cesium and nitrogen (3.03 Å).²⁵ As a result of the highly electropositive and polarisable nature of the large Cs⁺ ion, complex **6** crystallises as a polymeric species, in which the coordination environment of Cs1 is supplemented by the presence of six short Cs⋯C_(aryl) interactions²⁹ with the Ar–C centres of the six-membered aromatic backbone of an additional PDA framework, resulting in an η⁶-interaction [Cs1⋯C1A 3.465(11), Cs1⋯C2A 3.548(11), Cs1⋯C3A 3.583(13) Å] and construction of a one-dimensional polymer. Two additional short interactions are observed between the cesium centre and the isopropyl CH₃ groups of the second diamine framework [Cs1⋯C12A 3.573(17) Å]. The Cs⋯C distances compare well to Cs–N distances observed in similar compounds: [Cs(LH₃)(py)]_n [3.78(2), 3.42(2), 3.55(2) and 3.45(2) Å], [Cs₂(LH₃)₂(H₂O)]·CH₃CN [3.639(7), 3.518(7), 3.558(6) and 3.596(7) Å],²⁴ [Cs{HC(PPh₂NSiMe₃)₂}(DME)]₂ [3.763(4) Å],²⁶ and

[Cs{([Me₃Si]₂C)P-(C₆H₄CH₂NMe₂)₂}(toluene)]_n[3.545(2)–3.864(2) Å].³⁵ The fact that **6** crystallises as a polymeric species can be attributed to the larger radius of cesium compared to the preceding group 1 metals (Cs⁺ 1.65; Li⁺ 0.78, Na⁺ 0.98, K⁺ 1.33 Å).³³ It is possible that the large, electropositive cesium centre is too large to enable two cesium centres to be accommodated by the PDA ligand. Instead, the increased space around the cesium centre means that η⁶-interactions are favoured in order to satisfy the coordination requirements of cesium, and polymerisation occurs.

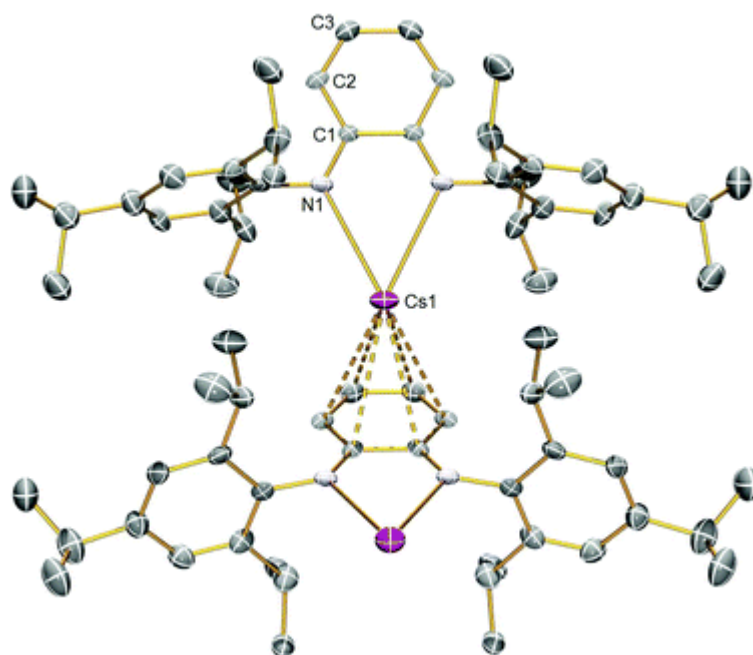


Fig. 4 Molecular structure of **6** with displacement ellipsoids set to 40% and selective labelling. Hydrogen atoms omitted for clarity.

Table 4 Selected bond lengths (Å) and angles (°) for **6**

Cs1–N1	2.985(9)
Cs1···C1A	3.465(11)
Cs1···C2A	3.548(11)
Cs1···C3A	3.583(13)
Cs1···C12A	3.573(17)
N1–C1	1.328(15)
N1–C4	1.409(15)
N1–Cs1–N1C	53.3(3)
Cs1–N1–C4	113.2(6)
Cs1–N1–C1	125.9(7)
C1–N1–C4	120.5(9)

The solid state structure of **6** supports the postulation of the formation of the analogous monorubidium salt **5**. Similar poly-hapto bonding would be expected to occur in **5**, affording a comparable polymeric species. In order to confirm that **5** and **6** are indeed radical anions as suggested by the structural and spectroscopic data, we probed **5** and **6** with EPR spectroscopy and DFT calculations.

The X-band EPR spectrum of **6** was initially recorded as a fluid solution in methyl-THF at ambient temperature. Hyperfine coupling was noted but the spectrum was weak and of insufficient resolution to allow the assignment of coupling. It is possible that this weak spectrum results from the propensity of **6** to form polymeric or oligomeric fragments in solution. Therefore, we added the tridentate ligand pentamethyldiethylenetriamine (PMDETA) to a solution of **6** in benzene in order to prevent such aggregation. This appeared to both increase the intensity and improve the resolution of the observed EPR spectrum, whilst retaining a similar linewidth (*ca.* 34 G) to that obtained without addition of PMDETA, suggesting that PMDETA acts to break up the polymeric chain into small, possibly monomeric units which are more amenable to study by EPR spectroscopy. Our best attempt to reproduce the experimental EPR spectrum by simulation was achieved using the parameters given in [Fig. 5](#). Simulations were improved, with respect to the number and position of lines, when the system was treated with asymmetric coupling to the nitrogen atoms and two of the hydrogen atoms ([Fig. 5](#)), however, reproduction of the experimental spectrum, with respect to the relative intensity of the constituent bands, was not obtained. Hence we present this as a tentative explanation of the coupling. No obvious ^{13}C s coupling is observed in the spectrum. The spectral width of 34 G is relatively narrow, and this, along with a *g* value of 2.004, is indicative of an organic free radical.

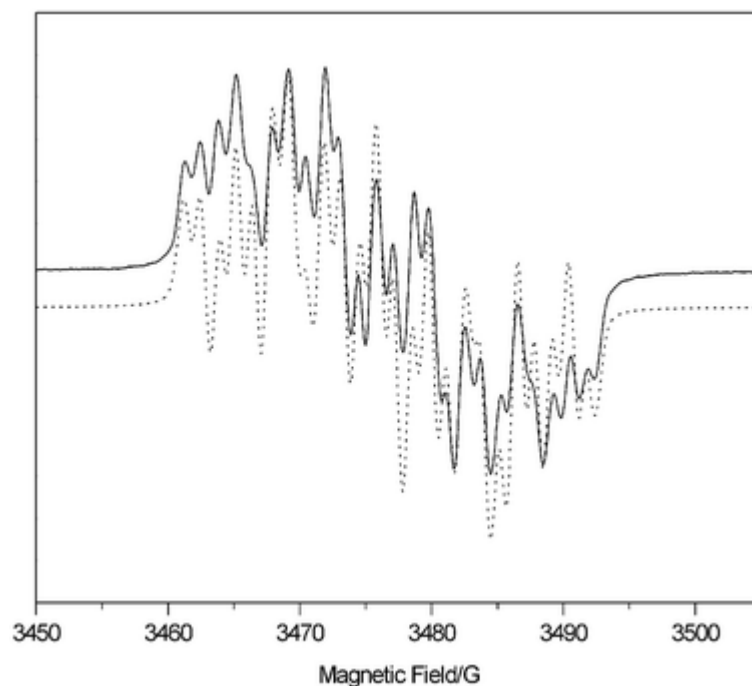


Fig. 5 X-band EPR spectrum of **6** in benzene solution containing PMDETA. Solid line: experimental; dotted line: simulation. Parameters used in the simulation: g_{iso} 2.004, a_{1H} 8 G, $a_{1H'}$ 7 G, a_{1N} 3.72 G, $a_{1N'}$ 2.72 G and a_{2H} 1.18 G, linewidth: 0.9 G and (0.50) lineshape.

The X-band EPR spectrum of **5** as a fluid solution at ambient temperature was also recorded in benzene containing PMDETA (Fig. 6), permitting comparisons with **6** to be made. For equivalent concentrations it was noted that the spectrum of **5** was significantly less intense than that of **6**. In an analogous manner to that observed for **6**, the addition of PMDETA to the solution of **5** improved the resolution of the subsequent EPR spectrum, suggesting that the complex is polymeric in solution and can be segmented by PMDETA. Comparison of the experimental spectrum for compound **5** with that obtained for **6** shows distinct similarities. The spectral width and g value are identical to the values obtained for **6** (34 G and 2.004), suggesting that the rubidium compound **5** is composed of a similar free radical, albeit with different constituent coupling given the difference in spectral profiles. It can therefore be concluded that **5** and **6** are radical anions. It is germane to note that the g values for **5** and **6** compare well to $[(\text{Et}_2\text{O})\text{Li}(\text{DippN})_2\text{C}_6\text{H}_4]$ ($g = 2.003$)²³ which is also deep green in solution, but the fine structure of the likely separated ion pairs **5** and **6** are different to the latter complex which remains as a contact ion pair in solution.

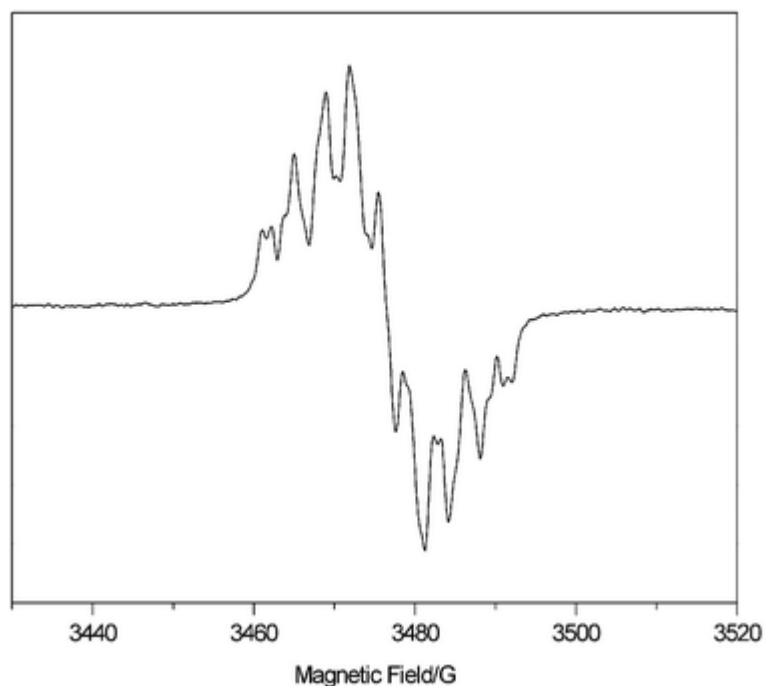


Fig. 6 Experimental X-band EPR spectrum of **5** in benzene solution containing PMDETA.

The EPR spectra suggest coupling of the free electron in **5** and **6** to nitrogen and hydrogen atoms which is supported by unrestricted DFT calculations using a ZORA/TZP all-electron basis set. We modelled the free radical anion since separated ion pairs are suggested by the EPR experiments. The Mulliken charges on the two nitrogen atoms were calculated to be -0.37 . Visual inspection of the SOMO ([Fig. 7](#)) gives some indication as to the position of electron density within the compound. The SOMO is localised on the two nitrogen atoms (41.4%) and the aromatic PDA backbone (46.4%), from which it can be concluded that the unpaired electron in the radical anion couples to two nitrogen (^{14}N , $I = 1$, 99.6%) and four hydrogen atoms (^1H , $I = 1/2$, 99.99%) as suggested by the EPR experiments.

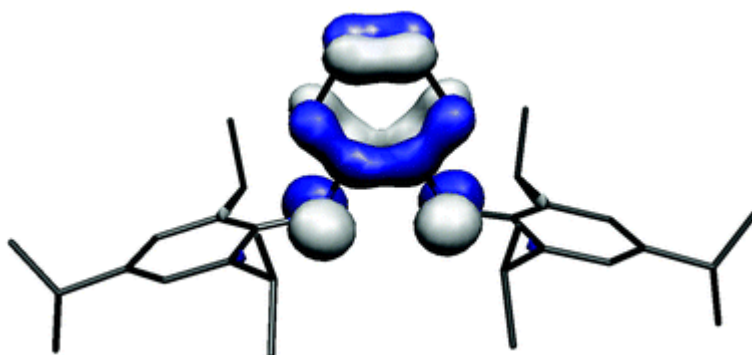


Fig. 7 SOMO (141a, 0.175 eV) for the radical anion of **5** and **6**.

Conclusions

A range of alkali metal PDA derivatives have been synthesised and isolated. As a consequence of the substantial range of ionic radii exhibited by the group 1 metals, a variety of structural arrangements are observed. The dilithium derivative adopts a monomeric structure, whereas the disodium and -potassium complexes adopt dimeric structures. In contrast, attempts to prepare the dirubidium and -cesium congeners resulted instead in the formation of monorubidium and -cesium radical anions. We are currently exploring the utility of the dilithium, -sodium, and -potassium salts in an improved synthesis of PDABBr.

Experimental

General

All manipulations were carried out using standard Schlenk and glovebox techniques, under an atmosphere of dry nitrogen. Solvents were dried by passage through activated alumina towers and degassed before use. All solvents were stored over potassium mirrors, with the exception of ethers, which were stored over activated 4 Å molecular sieves. Deuterated solvents were distilled from potassium, degassed by three freeze–pump–thaw cycles and stored under nitrogen. ^1H , ^{13}C , ^{31}P , ^7Li , and ^{11}B NMR spectra were recorded on a Bruker DPX/AV 400 spectrometer (operating at 400.2, 100.6, 162.0, 128.4, and 155.5 MHz, respectively). Chemical shifts are quoted in ppm and are relative to TMS (^1H and ^{13}C), external 85% H_3PO_4 (^{31}P), external 1.0 M LiCl (^7Li), and external 1.0 M $\text{BF}_3 \cdot \text{Et}_2\text{O}$ (^{11}B). FTIR spectra were recorded on a Bruker Tensor 27 FTIR spectrometer. EPR spectra were recorded at ambient temperature on an X-band Bruker EMX spectrometer fitted with a frequency counter. EPR spectral simulations were carried out using WINEPR SimFonia v1.25 software, Bruker Analytische Messtechnik GmbH. Elemental microanalysis was performed by Mr Stephen Boyer at the Microanalysis Service, London Metropolitan University, UK. *n*-Butyl lithium was purchased from Aldrich and was used as received. The compounds PDAH_2 ,¹⁹ $[\text{MCH}_2\text{C}_6\text{H}_5]$ ($\text{M} = \text{Na}–\text{Cs}$),^{41–44} and $[\text{MOC}_8\text{H}_{17}]$ ($\text{M} = \text{Rb}, \text{Cs}$)³⁵ were prepared by literature procedures.

Preparation of $[(\text{PDALi})_2(\text{THF})_3]$ (**2**)

A solution of *n*-butyl lithium (1.76 ml, 4.4 mmol; 2.5 M in hexanes) was added dropwise to a cold ($-78\text{ }^\circ\text{C}$) solution of **1** (1.03 g, 2.0 mmol) in THF (40 ml) with stirring and, after warming to room temperature, the resultant pale yellow solution was stirred for 24 hours. Removal of volatiles *in vacuo*, followed by recrystallisation from THF (3 ml) at $-30\text{ }^\circ\text{C}$ overnight yielded yellow-green crystals of **2** suitable for X-ray diffraction. Yield = 0.98 g, 94%. Anal. calc'd for $\text{C}_{48}\text{H}_{74}\text{Li}_2\text{N}_2\text{O}_3$: C, 77.80, H, 10.07, N, 3.78. Found: C, 77.68, H, 10.00, N, 3.84. ^1H NMR (C_6D_6 , 298 K): δ 1.47 (d, $^3J_{\text{HH}} = 6.8\text{ Hz}$, 12 H, $\text{CH}(\text{CH}_3)_2$), 1.55 (d, $^3J_{\text{HH}} = 6.8\text{ Hz}$, 12 H, $\text{CH}(\text{CH}_3)_2$), 1.56 (d, $^3J_{\text{HH}} = 6.8\text{ Hz}$, 12 H, $\text{CH}(\text{CH}_3)_2$), 3.17 (sept, $^3J_{\text{HH}} = 6.8\text{ Hz}$, 2 H, $\text{CH}(\text{CH}_3)_2$), 3.57 (sept, $^3J_{\text{HH}} = 6.8\text{ Hz}$, 4 H, $\text{CH}(\text{CH}_3)_2$), 6.43 (m, $^3J_{\text{HH}} = 3.6\text{ Hz}$, 2 H, Ar-*H*), 6.64 (m, $^3J_{\text{HH}} = 3.6\text{ Hz}$, 2 H, Ar-*H*), 7.46 (s, 4 H, Tripp-Ar-*H*). $^{13}\text{C}\{^1\text{H}\}$ NMR (C_6D_6 , 298 K): δ 25.21, 25.46, 26.05 ($\text{CH}(\text{CH}_3)_2$), 29.19, 35.19 ($\text{CH}(\text{CH}_3)_2$), 112.17, 115.03, 121.84 (Ar-CH), 140.64, 144.11, 148.79, 151.32 (Ar-C). ^7Li NMR (C_6D_6 , 298 K): δ 1.6 (s). FTIR ν/cm^{-1} (Nujol): 610 (w), 741 (m), 850 (w), 888 (w), 899 (w), 940 (w), 1038 (s), 1167 (m), 1206 (w), 1299 (m), 1404 (m), 1555 (s), 1590 (m), 1899 (w, br), 2018 (w), 3133 (m, br).

Preparation of $[\{(\text{PDANa})_2(\text{THF})_2\}_2]$ (**3**)

A solution of benzyl sodium (0.46 g, 4.0 mmol) in THF (10 ml) was added dropwise to a cold ($-78\text{ }^{\circ}\text{C}$) solution of **1** (1.03 g, 2.0 mmol) in THF (10 ml) with stirring and, after warming to room temperature, the resultant yellow-brown solution was stirred for 24 hours. Following removal of volatiles *in vacuo*, recrystallisation from toluene (18 ml) at $-30\text{ }^{\circ}\text{C}$ yielded orange crystals of **3** suitable for X-ray crystallographic analysis. Yield = 0.34 g, 24%. Anal. calc'd for $\text{C}_{88}\text{H}_{132}\text{Na}_2\text{N}_4\text{O}_4$: C, 75.39, H, 9.49, N, 4.00. Found: C, 75.21, H, 9.47, N, 3.92. ^1H NMR (d_8 -THF, 298 K): δ 1.06 (d, br, 12 H, $\text{CH}(\text{CH}_3)_2$), 1.10 (d, $^3J_{\text{HH}} = 6.8\text{ Hz}$, 24 H, $\text{CH}(\text{CH}_3)_2$), 1.17 (d, $^3J_{\text{HH}} = 6.8\text{ Hz}$, 12 H, $\text{CH}(\text{CH}_3)_2$), 1.22 (d, $^3J_{\text{HH}} = 6.8\text{ Hz}$, 12 H, $\text{CH}(\text{CH}_3)_2$), 1.26 (d, $^3J_{\text{HH}} = 6.8\text{ Hz}$, 12 H, $\text{CH}(\text{CH}_3)_2$), 2.86 (sept, $^3J_{\text{HH}} = 6.8\text{ Hz}$, 4 H, $\text{CH}(\text{CH}_3)_2$), 3.30 (s, br, 4 H, $\text{CH}(\text{CH}_3)_2$), 3.46 (sept, $^3J_{\text{HH}} = 6.8\text{ Hz}$, 4 H, $\text{CH}(\text{CH}_3)_2$), 5.72 (m, $^3J_{\text{HH}} = 3.6\text{ Hz}$, 6 H, Ar-*H*), 5.91 (m, $^3J_{\text{HH}} = 3.6\text{ Hz}$, 2 H, Ar-*H*), 6.82 (s, br, 4 H, Tripp-Ar-*H*), 6.98 (s, 4 H, Tripp-Ar-*H*). $^{13}\text{C}\{^1\text{H}\}$ NMR (d_8 -THF, 298 K): δ 23.90, 24.10, 24.30, 24.50, 24.70 ($\text{CH}(\text{CH}_3)_2$), 27.39, 34.16 ($\text{CH}(\text{CH}_3)_2$), 107.83, 108.92, 118.34, 118.65 (Ar-CH), 134.12, 139.77, 142.36, 149.32 (Ar-C). FTIR ν/cm^{-1} (Nujol): 588 (w), 640 (w), 741 (s), 898 (m), 941 (w), 1047 (m), 1165 (m), 1204 (w), 1278 (m), 1290 (m), 1530 (s), 1588 (w), 2029 (w), 3441 (w, br).

Preparation of $[\{(\text{PDAK}_2)(\text{THF})_3\}_2]$ (**4**)

A solution of benzyl potassium (0.26 g, 2.0 mmol) in THF (20 ml) was added dropwise to a cold ($-78\text{ }^{\circ}\text{C}$) solution of **1** (0.51 g, 1.0 mmol) in THF (20 ml) with stirring and, after warming to room temperature, the resultant deep orange solution was stirred for 72 hours. Removal of volatiles *in vacuo*, followed by recrystallisation from THF (5 ml) at $5\text{ }^{\circ}\text{C}$ overnight yielded green crystals of **4** suitable for X-ray diffraction. Yield = 0.39 g, 67%. Anal. calc'd for $\text{C}_{96}\text{H}_{148}\text{K}_4\text{N}_4\text{O}_6$: C, 71.61, H, 9.26, N, 3.48. Found: C, 71.50, H, 9.36, N, 3.51. ^1H NMR (d_8 -THF, 298 K): δ 1.00 (d, br, $^3J_{\text{HH}} = 6.8\text{ Hz}$, 12 H, $\text{CH}(\text{CH}_3)_2$), 1.13 (d, $^3J_{\text{HH}} = 6.8\text{ Hz}$, 12 H, $\text{CH}(\text{CH}_3)_2$), 1.16 (d, $^3J_{\text{HH}} = 6.8\text{ Hz}$, 12 H, $\text{CH}(\text{CH}_3)_2$), 1.22 (d, $^3J_{\text{HH}} = 6.8\text{ Hz}$, 24 H, $\text{CH}(\text{CH}_3)_2$), 1.26 (d, $^3J_{\text{HH}} = 6.8\text{ Hz}$, 12 H, $\text{CH}(\text{CH}_3)_2$), 2.85 (sept, br, $^3J_{\text{HH}} = 6.8\text{ Hz}$, 4 H, $\text{CH}(\text{CH}_3)_2$), 3.43 (sept, br, $^3J_{\text{HH}} = 6.8\text{ Hz}$, 8 H, $\text{CH}(\text{CH}_3)_2$), 5.70 (m, $^3J_{\text{HH}} = 3.6\text{ Hz}$, 8 H, Ar-*H*), 6.79 (s, br, 4 H, Tripp-Ar-*H*), 6.96 (s, 4 H, Tripp-Ar-*H*). $^{13}\text{C}\{^1\text{H}\}$ NMR (d_8 -THF, 298 K): δ 23.83, 24.11, 24.30, 24.50, 24.70 ($\text{CH}(\text{CH}_3)_2$), 27.45, 34.15 ($\text{CH}(\text{CH}_3)_2$), 108.06, 109.03, 111.97, 120.18 (Ar-CH), 141.20, 141.86, 143.71, 145.01 (Ar-C). FTIR ν/cm^{-1} (Nujol): 581 (w), 639 (w), 725 (s), 877 (m), 894 (m), 916 (w), 938 (w), 1046 (m), 1099 (m), 1115 (w), 1166 (m), 1282 (m), 1301 (w), 1405 (m), 1529 (s), 1606 (m, br), 1899 (w, br), 2028 (w), 3175 (s, br), 3416 (s, br).

Preparation of [PDARb] (**5**)

Method A. To a cold ($-78\text{ }^{\circ}\text{C}$) solution of **2** (0.74 g, 1.0 mmol) in THF (20 ml) a solution of rubidium 2-ethylhexoxide (1.0 ml, 2.0 mmol; 2 M soln in THF) was added, while stirring. The reaction mixture was allowed to warm to ambient temperature and the resultant dark green solution was stirred for 12 hours. Removal of volatiles *in vacuo*, followed by hexane washings yielded a dark green oil. Yield = 0.42 g, 70%. Several attempts to access single crystals suitable for X-ray crystallographic analysis, utilising a variety of solvents, a range of temperatures and a number of methods (*e.g.* slow diffusion), resulted only in the formation of microcrystalline material. Repeatable microanalysis results could not be obtained. NMR data were broad and uninformative. *Method B.* A solution of benzyl rubidium (0.18 g, 1.0 mmol) in THF (10 ml) was added dropwise to a cold ($-78\text{ }^{\circ}\text{C}$) solution of **1** (0.26 g, 0.5 mmol) in THF (10 ml) with stirring and, after warming to room temperature, the resultant yellow-green solution was stirred for 24 hours. Removal of volatiles *in vacuo* yielded a dark green oily solid. Yield = 0.22 g, 49%. Several attempts to access single crystals suitable for X-ray crystallographic analysis, utilising a variety of

solvents, a range of temperatures and a number of methods (*e.g.* slow diffusion), resulted only in the formation of microcrystalline material. NMR data were broad and uninformative.

Preparation of [PDACs]_n (**6**)

Method A. To a cold (−78 °C) solution of **2** (0.74 g, 1 mmol) in THF (20 ml) a solution of cesium 2-ethylhexoxide (2.0 ml, 2 mmol; 1 M soln in THF) was added, while stirring. The reaction mixture was allowed to warm to ambient temperature and the resultant emerald green solution was stirred for 12 hours. Removal of volatiles *in vacuo*, followed by hexane washings yielded an emerald green oil. Recrystallisation from toluene (20 ml) yielded colourless crystals of **6** suitable for X-ray crystallographic analysis. Yield = 0.34 g, 57%. Anal. calc'd for C₃₆H₅₀N₂Cs: C, 67.17, H, 7.83, N, 4.35. Found: C, 67.12, H, 7.72, N, 4.46. FTIR ν/cm^{-1} (Nujol): 528 (w), 589 (w), 649 (w), 669 (w), 742 (s), 765 (w), 844 (w), 876 (m), 891 (w), 944 (w), 1033 (m, br), 1162 (w, br), 1304 (w), 1338 (w), 1399 (m), 1499 (m), 1538 (w), 1598 (m), 1607 (m), 3353 (m). NMR data were broad and uninformative. *Method B.* A solution of benzyl cesium (0.22 g, 1.0 mmol) in THF (10 ml) was added dropwise to a cold (−78 °C) solution of **1** (0.26 g, 0.5 mmol) in THF (10 ml) with stirring and, after warming to room temperature, the resultant red-orange solution was stirred for 24 hours. Removal of volatiles *in vacuo*, yielded a green oily powder. Yield = 0.26 g, 52%. Several attempts to access X-ray quality crystals of **6**, utilising a variety of solvents, a range of temperatures and a number of methods (*e.g.* slow diffusion), resulted only in the formation of microcrystalline material. NMR data were broad and uninformative.

X-ray crystallography

Crystal data for compounds **2–4** and **6** are given in the ESI.† Bond lengths and angles are listed in [Tables 1–4](#). Crystals were examined on a Bruker APEX CCD area detector diffractometer using graphite-monochromated MoK α radiation ($\lambda = 0.71073 \text{ \AA}$), or on an Oxford Diffraction SuperNova Atlas CCD diffractometer using mirror-monochromated CuK α radiation ($\lambda = 1.5418 \text{ \AA}$). Intensities were integrated from data recorded on 0.3 (APEX) or 1° (SuperNova) frames by ω rotation. Cell parameters were refined from the observed positions of all strong reflections in each data set. Semi-empirical absorption correction based on symmetry-equivalent and repeat reflections (APEX) or Gaussian grid face-indexed absorption correction with a beam profile correction (SuperNova) were applied. The structures were solved variously by direct and heavy atom methods and were refined by full-matrix least-squares on all unique F^2 values, with anisotropic displacement parameters for all non-hydrogen atoms, and with constrained riding hydrogen geometries; $U_{\text{iso}}(\text{H})$ was set at 1.2 (1.5 for methyl groups) times U_{eq} of the parent atom. Programs were Bruker AXS SMART, and CrysAlisPro (control), Bruker AXS SAINT, and CrysAlisPro (integration), and SHELXTL and OLEX2 were employed for structure solution and refinement and for molecular graphics.^{45–48} Data are deposited with the CCDC numbers [961088–961091](#).

Density functional theory calculations


















Unrestricted geometry optimisations were performed on the radical anion component of **5** and **6** using coordinates derived from the experimental X-ray crystal structure of **6**. No constraints were imposed on the structure during the geometry optimisation. Calculations were performed using the Amsterdam Density Functional (ADF) suite version 2012.01.^{49,50} Slater type orbital (STO) triple- ζ -plus polarisation all-electron basis sets (from the ZORA/TZP database of the ADF suite) were employed. Scalar relativistic approaches were used within the ZORA Hamiltonian for the inclusion of relativistic effects and the local density approximation (LDA),


























with the correlation potential due to Vosko *et al.*⁵¹ used in all of the calculations. Gradient corrections were performed using the functionals of Becke⁵² and Perdew.⁵³ MOLEKEL⁵⁴ was used to prepare the three-dimensional plot of the electron density.













Acknowledgements

We thank the Royal Society, European Research Council, and University of Nottingham for supporting this work.

References

1. J. Koller and R. G. Bergman, *Chem. Commun.*, 2010, **46**, 4577 [RSC](#) .
2. J. V. Dickschat, S. Urban, T. Pape, F. Glorius and F. E. Hahn, *Dalton Trans.*, 2010, **39**, 11519 [RSC](#) .
3. M. M. Khusniyarov, K. Harms, O. Burghaus, J. Sundermeyer, B. Sarkar, W. Kaim, J. van Slageren, C. Duboc and J. Fiedler, *Dalton Trans.*, 2008, 1355 [RSC](#) .
4. M. M. Khusniyarov, T. Weyhermüller, E. Bill and K. Wieghardt, *J. Am. Chem. Soc.*, 2009, **131**, 1208 [CrossRef](#) [CAS](#) [PubMed](#) .
5. N. A. Ketterer, H. Fan, K. J. Blackmore, X. Yang, J. W. Ziller, M. Baik and A. F. Heyduk, *J. Am. Chem. Soc.*, 2008, **130**, 4364 [CrossRef](#) [CAS](#) [PubMed](#) .
6. M. M. Khusniyarov, E. Bill, T. Weyhermüller, E. Bothe, K. Harms, J. Sundermeyer and K. Wieghardt, *Chem.–Eur. J.*, 2008, **14**, 7608 [CrossRef](#) [CAS](#) [PubMed](#) .
7. K. Chłopek, E. Bothe, F. Neese, T. Weyhermüller and K. Wieghardt, *Inorg. Chem.*, 2006, **45**, 6298 [CrossRef](#) [PubMed](#) .
8. G. Buncic, Z. Xiao, S. C. Drew, J. M. White, A. G. Wedd and P. S. Donnelly, *Chem. Commun.*, 2012, **48**, 2570 [RSC](#) .
9. M. M. Khusniyarov, T. Weyhermüller, E. Bill and K. Wieghardt, *Angew. Chem., Int. Ed.*, 2008, **47**, 1228 [CrossRef](#) [CAS](#) [PubMed](#) .
10. A. L. Balch, F. Röhrscheid and R. H. Holm, *J. Am. Chem. Soc.*, 1965, **87**, 2301 [CrossRef](#) [CAS](#) .
11. A. L. Balch and R. H. Holm, *J. Am. Chem. Soc.*, 1966, **88**, 5201 [CrossRef](#) [CAS](#) .
12. Y. Segawa, M. Yamashita and K. Nozaki, *Science*, 2006, **314**, 113 [CrossRef](#) [CAS](#) [PubMed](#) .
13. Y. Segawa, M. Yamashita and K. Nozaki, *Angew. Chem., Int. Ed.*, 2007, **46**, 6710 [CrossRef](#) [CAS](#) [PubMed](#) .
14. M. Yamashita, Y. Suzuki, Y. Segawa and K. Nozaki, *J. Am. Chem. Soc.*, 2007, **129**, 9570 [CrossRef](#) [CAS](#) [PubMed](#) .
15. Y. Segawa, Y. Suzuki, M. Yamashita and K. Nozaki, *J. Am. Chem. Soc.*, 2008, **130**, 16069 [CrossRef](#) [CAS](#) [PubMed](#) .
16. A. V. Protchenko, L. M. A. Saleh, D. Vidovic, D. Dange, C. Jones, P. Mountford and S. Aldridge, *Chem. Commun.*, 2010, **46**, 8546 [RSC](#) .
17. L. M. A. Saleh, K. H. Birj Kumar, A. V. Protchenko, A. D. Schwarz, S. Aldridge, C. Jones, N. Kaltosyannis and P. Mountford, *J. Am. Chem. Soc.*, 2011, **133**, 3836 [CrossRef](#) [CAS](#) [PubMed](#) .

18. T. Wenderski, K. M. Light, D. Ogrin, S. G. Bott and C. J. Harlan, *Tetrahedron Lett.*, 2004, **45**, 6851 [CrossRef](#) [CAS](#) [PubMed](#) 
19. S. Robinson, J. McMaster, W. Lewis, A. J. Blake and S. T. Liddle, *Chem. Commun.*, 2012, **48**, 5769 [RSC](#) 
20. As evidenced from a search of the Cambridge Structural Database (CSD version 1.11, date: 15/09/2013): F. H. Allen, *Acta Crystallogr., Sect. B: Struct. Sci.*, 2002, **58**, 380 [CrossRef](#) [PubMed](#) 
21. S. Daniele, C. Drost, B. Gehrhus, S. M. Hawkins, P. B. Hitchcock, M. F. Lappert, P. G. Merle and S. G. Bott, *J. Chem. Soc., Dalton Trans.*, 2001, 3179 [RSC](#) 
22. P. B. Hitchcock, M. F. Lappert and X.-H. Wei, *Dalton Trans.*, 2006, 1181 [RSC](#) 
23. T. Janes, J. M. Rawson and D. Song, *Dalton Trans.*, 2013, **42**, 10640 [RSC](#) 
24. P. Thuery, Z. Asfari, J. Vicens, V. Lamare and J. Dozol, *Polyhedron*, 2002, **21**, 2497 [CrossRef](#) [CAS](#) 
25. P. Pyykkö and M. Atsumi, *Chem.–Eur. J.*, 2009, **15**, 186 [CrossRef](#) [PubMed](#) 
26. A. J. Wooles, M. Gregson, O. J. Cooper, A. Middleton-Gear, D. P. Mills, W. Lewis, A. J. Blake and S. T. Liddle, *Organometallics*, 2011, **30**, 5314 [CrossRef](#) [CAS](#) 
27. W. Clegg, E. K. Cope, A. J. Edwards and F. S. Mair, *Inorg. Chem.*, 1998, **37**, 2317 [CrossRef](#) [CAS](#) 
28. G. W. Rabe, S. Kheradmandan and G. P. A. Yap, *Inorg. Chem.*, 1998, **37**, 6541 [CrossRef](#) [CAS](#) 
29. K. W. Klinkhammer, *Chem.–Eur. J.*, 1997, **3**, 1418 [CrossRef](#) [CAS](#) 
30. G. C. Forbes, A. R. Kennedy, R. E. Mulvey, B. A. Roberts and R. B. Rowlings, *Organometallics*, 2002, **21**, 5115 [CrossRef](#) [CAS](#) 
31. S. T. Liddle and P. L. Arnold, *Dalton Trans.*, 2007, 3305 [RSC](#) 
32. G. W. Gokel, S. L. De Wall and E. S. Meadows, *Eur. J. Org. Chem.*, 2000, 2967 [CrossRef](#) [CAS](#) 
33. J. Emsley, *The Elements*, Oxford University Press, New York, 1st edn, 1989 [Search PubMed](#) 
34. L. Wing-Por, C. Hui, L. Dian-Sheng, W. Qi-Guang and T. C. W. Mak, *Organometallics*, 2000, **19**, 3001 [CrossRef](#) 
35. K. Izod, W. Clegg and S. T. Liddle, *Organometallics*, 2001, **20**, 367 [CrossRef](#) [CAS](#) 
36. A. J. Wooles, M. Gregson, S. Robinson, O. J. Cooper, D. P. Mills, W. Lewis, A. J. Blake and S. T. Liddle, *Organometallics*, 2011, **30**, 5326 [CrossRef](#) [CAS](#) 
37. A. J. Wooles, D. P. Mills, W. Lewis, A. J. Blake and S. T. Liddle, *Dalton Trans.*, 2010, **39**, 500 [RSC](#) 
38. R. J. Baker, R. D. Farley, C. Jones, M. Kloth and D. M. Murphy, *J. Chem. Soc., Dalton Trans.*, 2002, 3844 [RSC](#) 
39. R. J. Baker, R. D. Farley, C. Jones, D. P. Mills, M. Kloth and D. M. Murphy, *Chem.–Eur. J.*, 2005, **11**, 2972 [CrossRef](#) [CAS](#) [PubMed](#) 
40. W. Clegg, A. R. Kennedy, J. Klett, R. E. Mulvey and L. Russo, *Eur. J. Inorg. Chem.*, 2012, 2989 [CrossRef](#) [CAS](#) 
41. L. Orzechowski, G. Jansen and S. Harder, *Angew. Chem., Int. Ed.*, 2009, **48**, 3825 [CrossRef](#) [CAS](#) [PubMed](#) 
42. M. Schlosser and J. Hartmann, *Angew. Chem., Int. Ed. Engl.*, 1973, **12**, 508 [CrossRef](#) 

43. S. H. Bertz, C. P. Gibson and G. Dabbagh, *Organometallics*, 1988, **7**, 227 [CrossRef](#) [CAS](#) 
44. D. Hoffmann, W. Bauer, F. Hampel, N. J. R. van Eikema Hommes, P. von, R. Schleyer, P. Otto, U. Pieper, D. Stalke, D. S. Wright and R. Snaith, *J. Am. Chem. Soc.*, 1994, **116**, 528 [CrossRef](#) [CAS](#) 
45. *SMART and SAINT*, Bruker AXS Inc., Madison, WI, USA, 2001 [Search PubMed](#) 
46. *CrysAlis PRO*, Agilent Technologies, Yarnton, England, 2010 [Search PubMed](#) 
47. G. M. Sheldrick, *Acta Crystallogr., Sect. A: Fundam. Crystallogr.*, 2008, **64**, 112 [CrossRef](#) [CAS](#) [PubMed](#) 
48. O. V. Dolomanov, L. J. Bourhis, R. J. Gildea, J. A. K. Howard and H. Puschmann, *J. Appl. Crystallogr.*, 2009, **42**, 339 [CrossRef](#) [CAS](#) 
49. C. Fonseca-Guerra, J. G. Snijders, G. te Velde and E. J. Baerends, *Theor. Chem. Acc.*, 1998, **99**, 391 [Search PubMed](#) 
50. G. Te Velde, F. M. Bickelhaupt, S. J. A. Van Gisbergen, C. Fonseca-Guerra, E. J. Baerends, J. G. Snijders and T. Ziegler, *J. Comput. Chem.*, 2001, **22**, 931 [CrossRef](#) [CAS](#) 
51. S. H. Vosko, L. Wilk and M. Nusair, *Can. J. Phys.*, 1980, **58**, 1200 [CrossRef](#) [CAS](#) [PubMed](#) 
52. A. D. Becke, *Phys. Rev. A*, 1988, **38**, 3098 [CrossRef](#) [CAS](#) 
53. J. P. Perdew, *Phys. Rev. B: Condens. Matter*, 1986, **33**, 8822 [CrossRef](#) 
54. F. M. Bickelhaupt, N. M. van Nibbering, E. M. Wezenbeek and E. J. Baerends, *J. Phys. Chem.*, 1992, **96**, 4864 [CrossRef](#) [CAS](#) 

Footnote

† Electronic supplementary information (ESI) available: X-ray crystallographic data for **2–4** and **6** and final coordinates and energy for the radical **961091**. For ESI and crystallographic data in CIF or other electronic format see DOI: [10.1039/c3dt52632a](https://doi.org/10.1039/c3dt52632a)